Supporting Information

Mineralization of macroaggregated albumin for accurate biodistribution evaluation of pre-radiotherapy

Xiaomin Gao,[‡,a,b] Mingru Zhang,[‡,c] Danlan Fang,[‡,d] Yuan Yu,[*,e] Shaolong Qi,[b] Xinyang Yu,[b] Meiqi Cheng,[b] Shoujun Zhu,[d] Fei Kang,[*,c] Kuikun Yang,[*,a] and Guocan Yu[*,b]

[a] Faculty of Life Science and Medicine, School of Life Science and Technology, Harbin Institute of Technology Harbin, Heilongjiang 150080, P. R. China.

[b] Key Laboratory of Bioorganic Phosphorus Chemistry & Chemical Biology, Department of Chemistry, Tsinghua University, Beijing 100084, P. R. China

[c] Department of Nuclear Medicine, Xijing Hospital, Fourth Military Medical University, Xi'an, Shaanxi, 710032, P. R. China

[d] State Key Laboratory of Supramolecular Structure and Materials, Center for Supramolecular Chemical Biology, College of Chemistry, Jilin University, Changchun, 130012, China

[e] Zhejiang Provincial Key Laboratory of Fiber Materials and Manufacturing Technology, Zhejiang Sci-Tech University, Hangzhou 310018, P.R. China

[#] X. Gao, M. Zhang, and D. Fang contribute equally to this work.

[*] Corresponding authors: yuyu@zstu.edu.cn (Y. Yu); fmmukf@qq.com (F. Kang); yangkuikun@hit.edu.cn (K. Yang); guocanyu@mail.tsinghua.edu.cn (G. Yu).

Experimental Section

Materials. HSA was purchased from Psaitong Biotechnology Co., Ltd, glutaraldehyde was purchased from Energy Chemical. Sodium acetate anhydrous was purchased from the DAMAO chemical reagent factory. 2,3,3-trimethyl-3H-indole, 1-Iodohexadecane, phosphors oxychloride, cyclohexanone, toluene, acetonitrile, diethyl ether, petroleum ether, methanol, and benzene were purchased from TCI and Sigma Aldrich. All reagents were commercially available and were used as supplied without further purification.

Synthesis of ICG-C16 (indocyanine green modified palmitic acid)

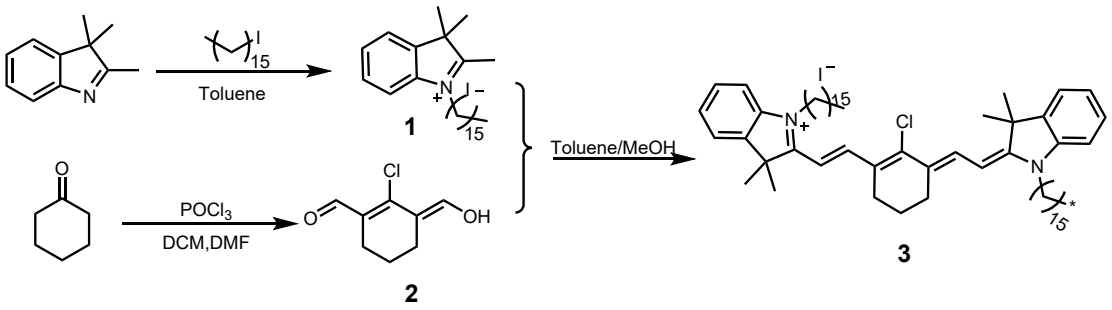

Fig. S1. Synthesis route of ICG-C16.

Synthesis of compound 1.

A solution of 2,3,3-trimethyl-3H-indole (2.5 g, 15.7 mmol) in toluene and acetonitrile (200 mL, 1:1) was stirred. 1-Iodohexadecane (16.6 g, 47.1 mmol) was added to the solution at room temperature, and the mixture was stirred at 90°C for 15 h. After cooling the mixture to room temperature, it was added dropwise to cold diethyl ether. The red precipitate was collected and washed with 200 mL of petroleum ether. Finally, the residue was purified by flash column chromatography using DCM/MeOH (50:1, v/v) to obtain pale purple solid.

Synthesis of compound 2.

A solution of DMF (7.33 g, 7.7 mL, 100 mmol) in DCM (10 mL) was added dropwise to a stirred solution of phosphorus oxychloride (15.62 g, 101.89 mmol) in DCM (100 mL). After 30 min, cyclohexanone (5 g, 50.95 mmol) in 10 mL of DCM was added and the mixture was stirred at 80°C for 4 h. The mixture was then cooled to room temperature and poured into cold water. It was stirred overnight and the solid product was obtained by filtration.

Synthesis of compound 3.

Compound 2 (2.3 g, 13.4 mmol) was added to a stirred solution of compound 1 (8.4 g, 26.7 mmol) in a mixture of methanol and benzene (100 mL, 1:1) at room temperature. The mixture was refluxed for 12 h to give a dark green solution. The solvent was removed under reduced pressure to obtain the crude product. The crude product was purified by silica gel column chromatography using DCM/MeOH (20:1, v/v) to obtain green solid.

Preparation of MAA

A solution was prepared by dissolving human serum albumin (HSA) (20 mg) in physiological saline (0.9% NaCl, 0.4 mL). Subsequently, deionized water (0.4 mL), acetic acid/sodium acetate buffer (pH = 5.0, 0.2 mL), and glutaraldehyde solution (0.1%, 0.2 mL) were added to the solution at room temperature. The mixture was then stirred at 1100 rpm while the temperature was gradually increased to 80°C over 40 min. After maintaining the temperature at 80°C for 10 min, stirring was stopped and the reaction mixture was allowed to cool naturally to room temperature. The mixture was centrifuged at 3000 rpm for 3 min, the supernatant was discarded and the

precipitate was washed with water three times to obtain MAA.

Mineralization of MAA

L-MAA and H-MAA were prepared using the standard methodology. In summary, MAA was suspended in 1 mL of deionized water and 1 mL of $CaCl_2$ (30 mM or 100 mM) was added at room temperature. The mixture was stirred at room temperature at 150 rpm for 1 h after which 0.2 mL of Na_2CO_3 (1 mol L^{-1}) was added, the resulting mixture was stirred for another 1 h before the reaction was stopped. Subsequently, the mixture was washed with water three times to obtain L-MAA or H-MAA. The preparation of Re-L-MAA, Re-H-MAA, ^{99m}Tc-L-MAA, and ^{99m}Tc-H-MAA followed a method analogous to the mineralization of MAA.

^{99m}Tc-labeling of MAA

The MAA was dispersed in an aqueous solution (10 mg mL^{-1}) and treated with a stannous chloride solution (1 mg mL^{-1}) containing hydrochloric acid. Subsequently, a solution of $Na^{99m}TcO_4$ was added and the mixture was stirred for 30 min at room temperature. The mixture was washed three times with water to obtain ^{99m}Tc-MAA. The radiochemical purity was tested by a Mini-Scan radio-TLC Scanner (BioScan, USA). The radioactivity was measured with a γ-counter (WIZARD 2470, PerkinElmer, USA).

Re(rhenium)-labeling of MAA

The MAA was dispersed in an aqueous solution (10 mg mL^{-1}) and treated with a stannous chloride solution (1 mg mL^{-1}) containing hydrochloric acid. Subsequently, a solution of sodium perrhenate ($NaReO_4$) was added and stirred for 30 min at room temperature. The mixture was washed with water three times to obtain Re-MAA.

Preparation of silicon dioxide microspheres (SiO_2) and polymer microspheres (PMS).

SiO_2 microspheres: 5 g of TEOS-40 and 2 mL of hydrochloric acid (3 mol L^{-1}) were added into 25 mL of anhydrous ethanol in a round-bottom flask. The mixture was stirred at room temperature for 90 min. Subsequently, 20 mL of deionized water was added to the reaction solution, and the solution was vacuum-distilled until the volume reached 10 mL. In another round-bottom flask, 1.5 mL of methyl cellulose (1.4 wt%) and 1.5 mL of OP-10 in benzyl alcohol (19 vt%) were added into 20 mL of benzyl alcohol. 5 mL of the aforementioned aqueous silica source was introduced into the reaction system, The mixture was stirred for 15 min and then all water was removed by rotary evaporation at 70°C. The resulting product was filtered and washed with deionized water and ethanol to obtain SiO_2 microspheres.

Polymer microspheres (PMS): first, 0.4 g of PLA and 0.1 g of PLGA were dissolved in 1.5 mL of dichloromethane, while a 20 mL solution of polyvinyl alcohol (PVA) with a concentration of 1.5% was prepared. Subsequently, the PLA, PLGA, and PVA were mixed in a beaker and mechanically stirred at a speed of 750 rpm for 7 min. Thereafter, the blended solution was transferred to a fume hood and left to stand for 3 h to allow the organic solvent to evaporate. Following washing with ethanol and water, the product was ready for use.[1, 2]

NIR-II fluorescence imaging

Mice were anesthetized using isoflurane before placing them on a stage for injection of imaging agents. All NIR-II images were collected on a two-dimensional InGaAs camera (Princeton Instruments and Raptor Photonics) platform. The excitation laser was an 808 nm laser set up at a power density of ~78 mW cm^{-2}. Variable exposure time was used for the camera to capture images in the sub-NIR-II windows. NIR-II bioimaging were visualized under 1100 nm long pass filter with continuous laser exposure.

Small Animal Micro-SPECT/CT Imaging

The BALB/c female mice (15–20 g, 4–6 weeks old) were intravenously injected with approximately 0.5 mCi of ^{99m}Tc-MAA, either as ^{99m}Tc-L-MAA or ^{99m}Tc-H-MAA. The mice were anesthetized with isoflurane (2% mixed with air, 1.5 L min^{-1}), and scans were performed at 0.5, 2, and 6 h. Imaging was conducted using a high-energy mouse collimator with a 3.6 mm diameter pinhole. The central field of view of the collimator was approximately 28 mm in diameter and 18 mm in length. All generated SPECT and CT images were reconstructed using the PMOD software provided by the manufacturer. SPECT images were reconstructed with a 0.8 mm wide cubic voxel using a 20% energy window centered at 364 keV. A total of 6 iterations and 128 subsets were applied to all scans. Correction for Compton photon scattering and background signals was performed using a three-window method, employing two adjacent background scatter windows of approximately 5% width each. All animal experiments strictly complied with the standards of the Institutional Animal Care and Use Committee of Tsinghua University (protocol No. 21-YGC1.G24-1).

Blood analysis and measurement of serum levels of inflammatory cytokines with ELISA.

Twelve mice were randomly divided into four groups (n = 3) and intravenously administered 150 μL of (i) PBS, (ii) MAA, (iii) L-MAA, and (iv) H-MAA. After 7 days of treatment, blood samples were collected from the mice and analyzed using an automated hematology analyzer (Sysmex KX-21, Sysmex Co., Japan). The concentrations of inflammatory cytokines IL-6 in the serum were measured by ELISA using the kits purchased from Elabscience Biotechnology.

Statistical analysis

Data were presented as the means ± standard deviations (S.D) of at least three replicates. Statistical analysis was conducted by using GraphPad Prism 10.0. Statistical significance was calculated using one-way analysis of variance (ANOVA) or test when performing multiple comparisons between groups (*P < 0.05; **P < 0.01; ***P < 0.001; “ns” denoted no significant difference).

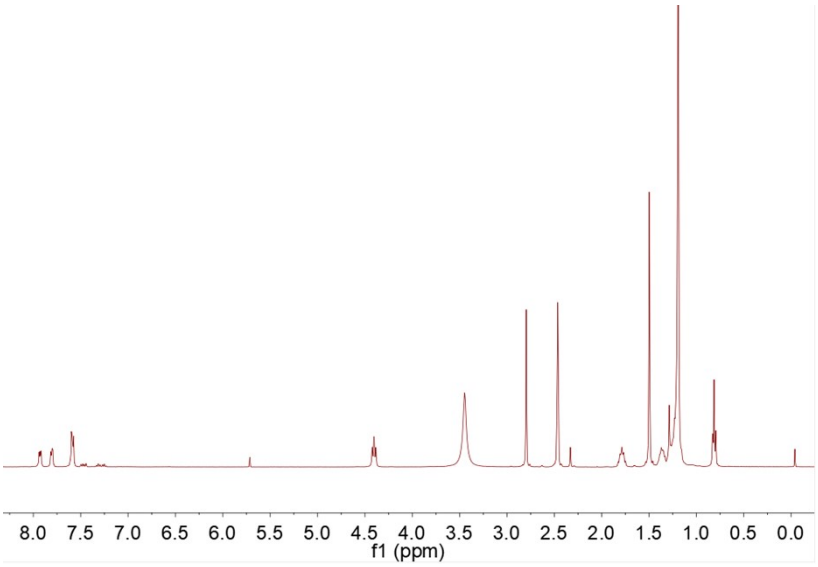

Fig. S2. ^{1}H NMR spectrum (400 MHz, DMSO-d6, room temperature) of compound 1.

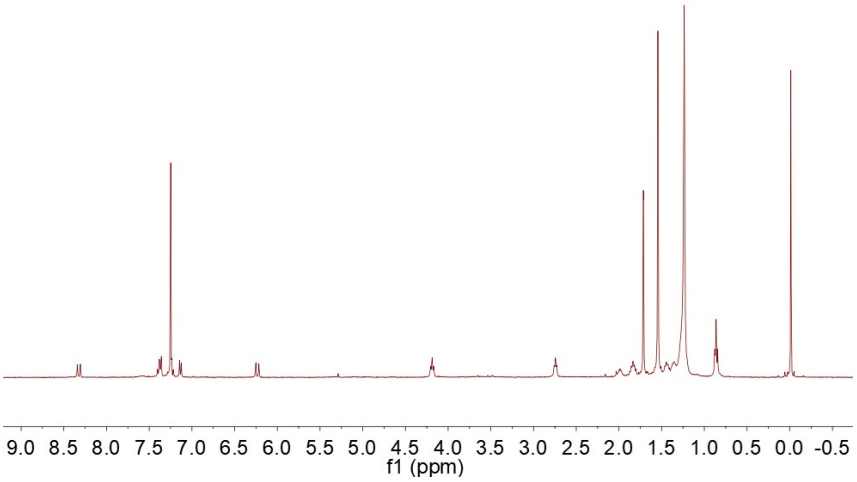

Fig. S3. ^{1}H NMR spectrum (400 MHz, $CDCl_3$, room temperature) of compound 3.

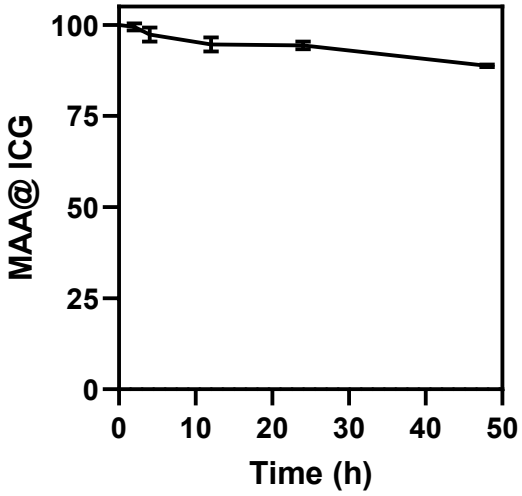

Fig. S4. The absorption changes of MAA@ICG after 48 h incubation in PBS containing 10% of fetal bovine serum.

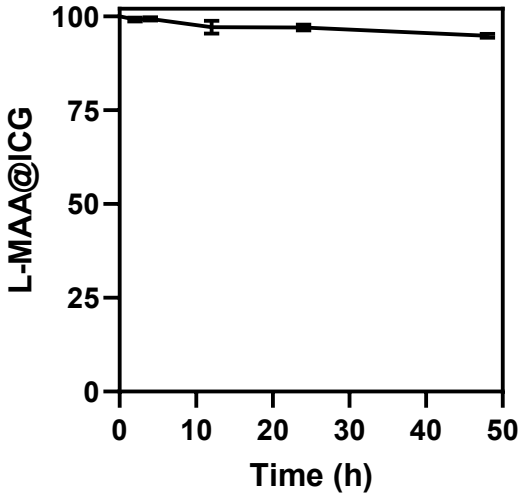

Fig. S5. The absorption changes of L-MAA@ICG after 48 h incubation in PBS containing 10% of fetal bovine serum.

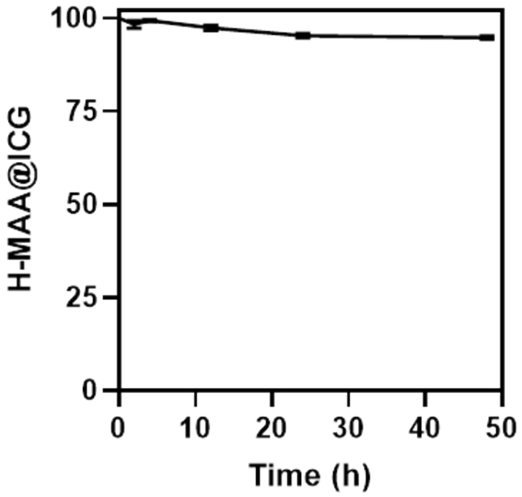

Fig. S6. The absorption changes of H-MAA@ICG after 48 h incubation in PBS containing 10% of fetal bovine serum.

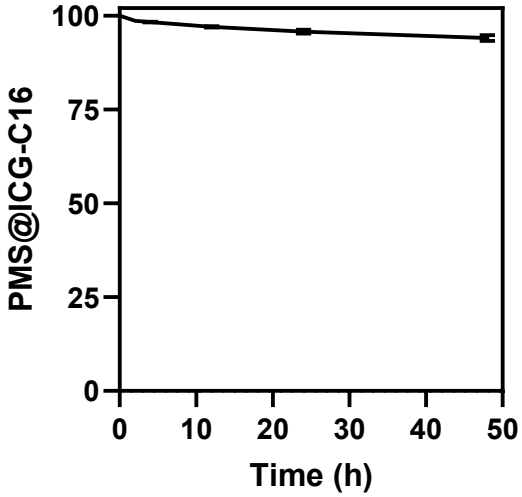

Fig. S7. The absorption changes of PMS@ICG-C16 after 48 h incubation in PBS containing 10% of fetal bovine serum.

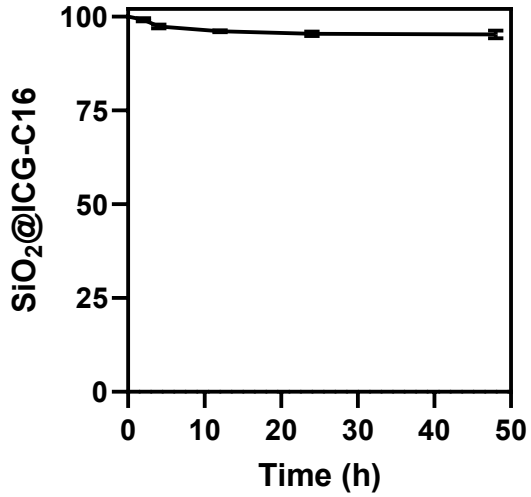

Fig. S8. The absorption changes of SiO_2@ICG-C16 after 48 h incubation in PBS containing 10% of fetal bovine serum.

	Injected activity (μci)	Radiochemical purity (%)
^{99m}Tc-MAA	521 ± 40	> 95%
^{99m}Tc-L-MAA	530 ± 30	> 95%
^{99m}Tc-H-MAA	490 ± 20	> 95%

Fig. S9. Activity of injection and radiochemical purity of MAA and mineralized MAA (L-MAA and H-MAA).

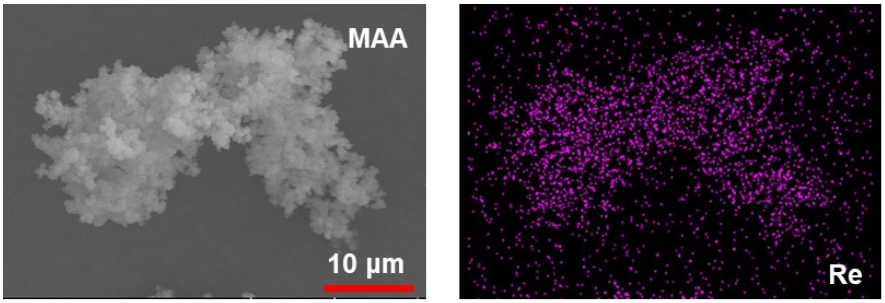

Fig. S10. SEM and the corresponding EDS spectroscopy elemental mapping images of Re-MAA.

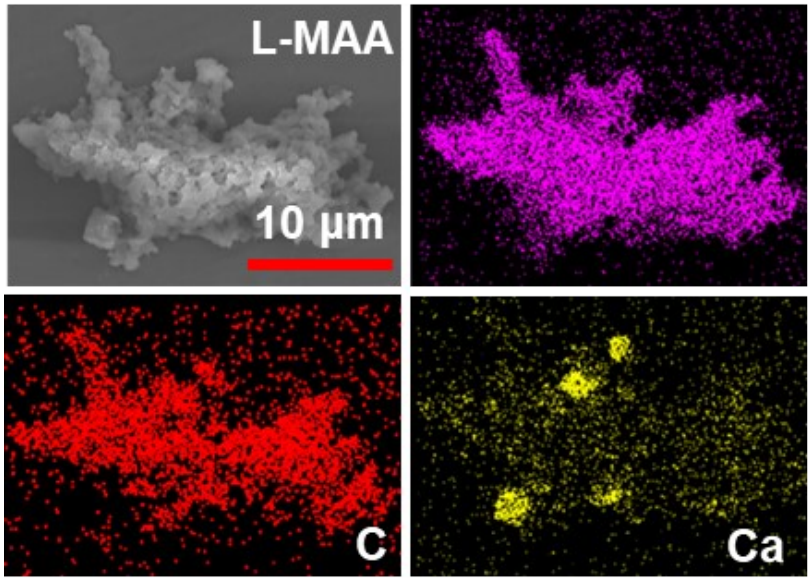

Fig. S11. SEM and the corresponding EDS spectroscopy elemental mapping images of Re-L-MAA.

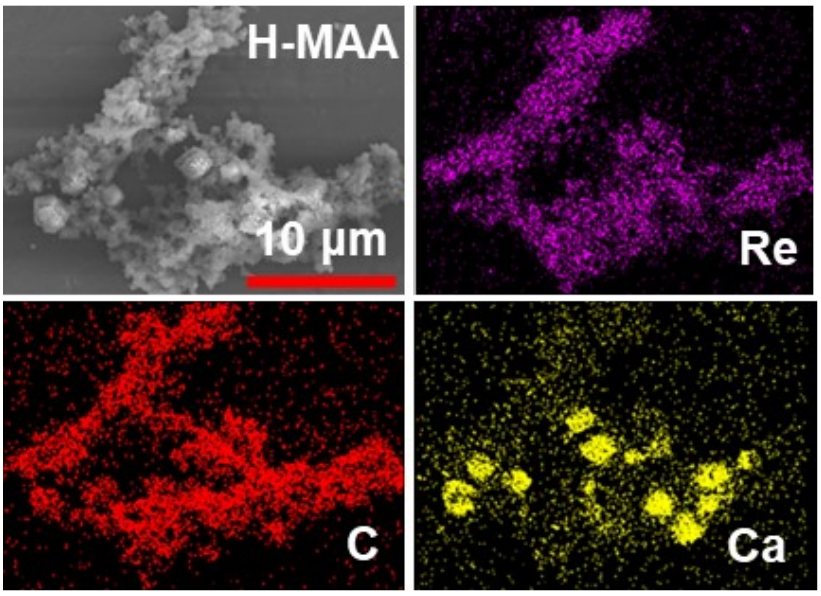

Fig. S12. SEM and the corresponding EDS spectroscopy elemental mapping images of Re-H-MAA.

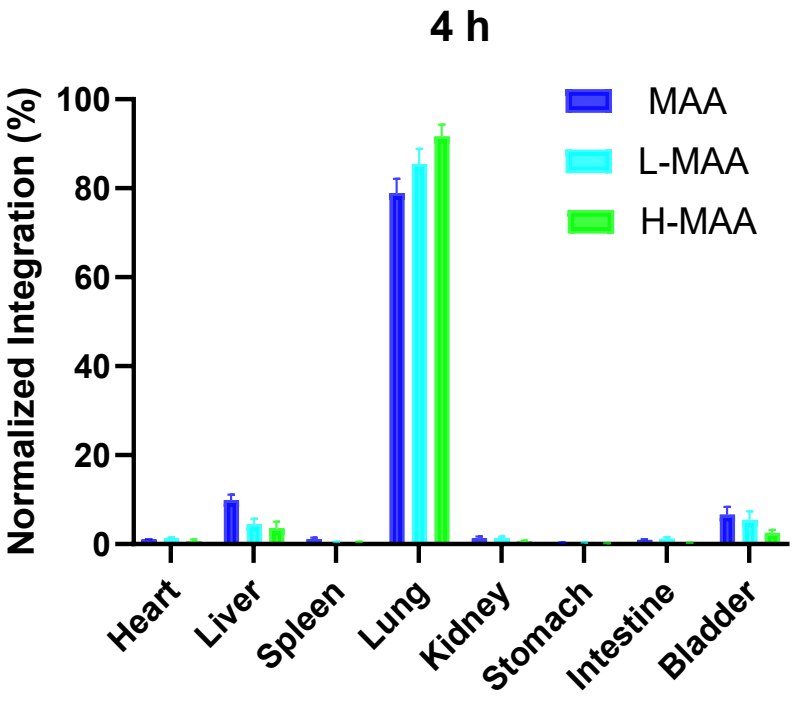

Fig. S13. Biodistribution of MAA and mineralized MAA (L-MAA and H-MAA) at 4 h after i.v. injection determined by ICP-MS.

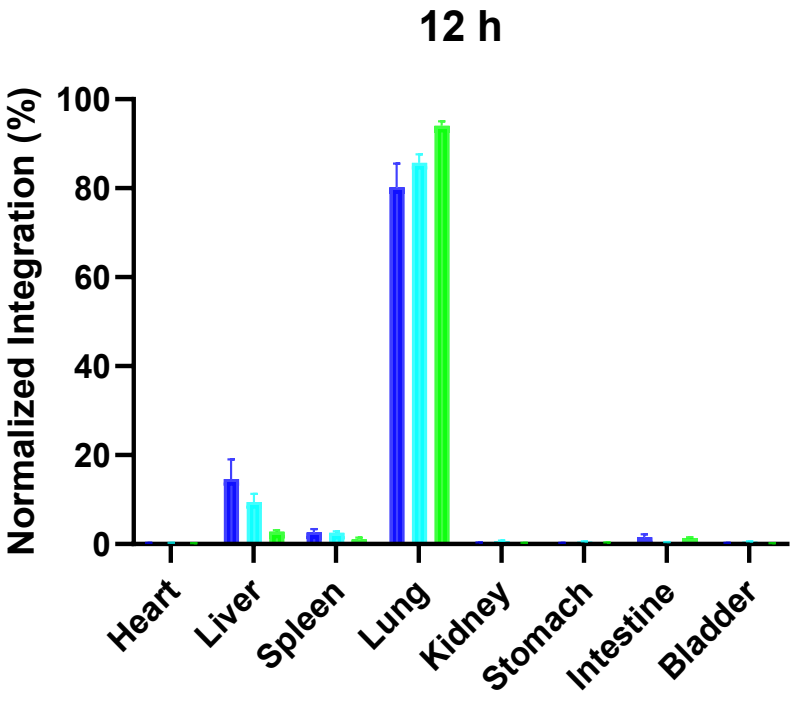

Fig. S14 Biodistribution of MAA and mineralized MAA (L-MAA and H-MAA) at 12 h after i.v. injection determined by ICP-MS.

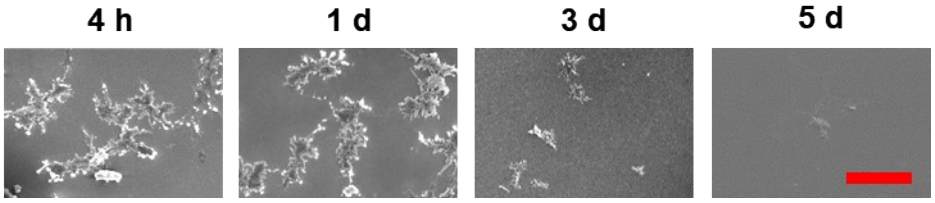

Fig. S15. The evaluation results on biodegradability of MAA. SEM images of MAA at pH = 5.5 at different times. Scale bar: 20 μm.

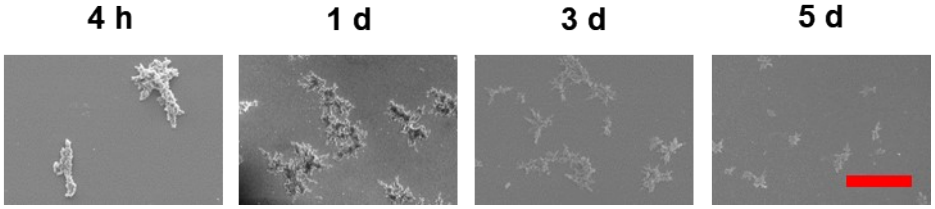

Fig. S16. The evaluation results on biodegradability of MAA. SEM images of MAA at pH = 6.5 at different times. Scale bar: 20 μm.

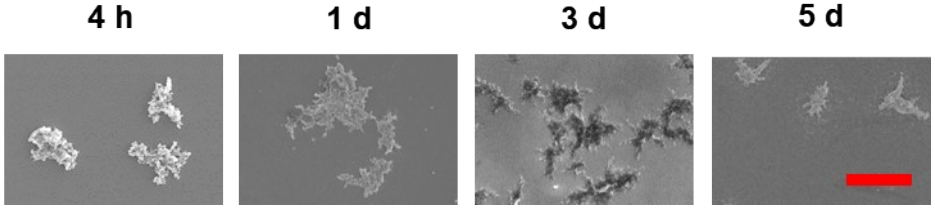

Fig. S17. The evaluation results on biodegradability of MAA. SEM images of MAA at pH = 7.4 at different times. Scale bar: 20 μm.

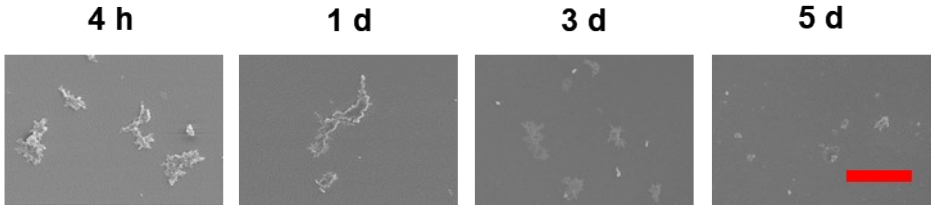

Fig. S18. The evaluation results on biodegradability of L-MAA. SEM images of L-MAA at pH = 5.5 at different times. Scale bar: 20 μm.

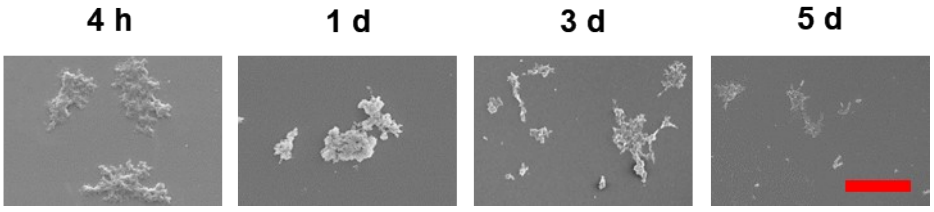

Fig. S19. The evaluation results on biodegradability of L-MAA. SEM images of L-MAA at pH = 6.5 at different times. Scale bar: 20 μm.

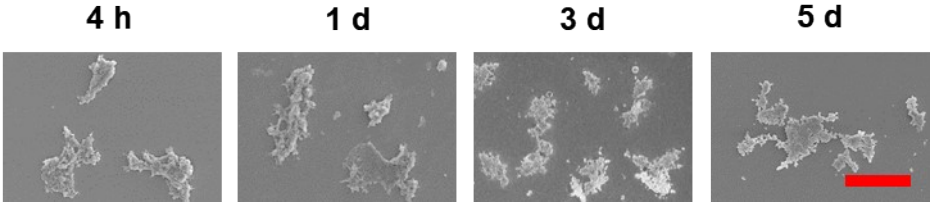

Fig. S20. The evaluation results on biodegradability of L-MAA. SEM images of L-MAA at pH = 7.4 at different times. Scale bar: 20 μm.

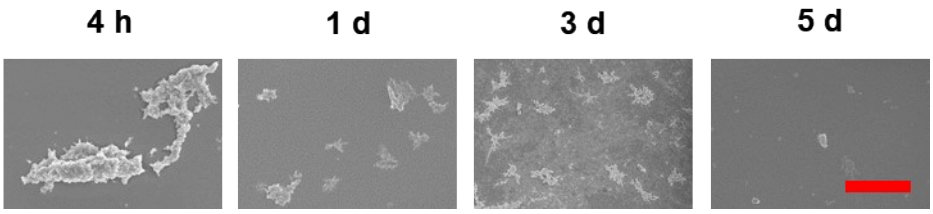

Fig. S21. The evaluation results on biodegradability of H-MAA. SEM images of H-MAA at pH = 5.5 at different times. Scale bar: 20 μm.

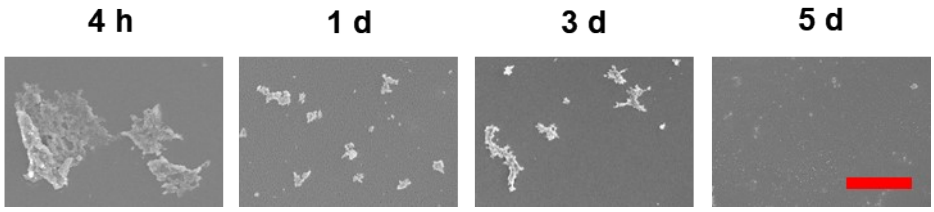

Fig. S22. The evaluation results on biodegradability of H-MAA. SEM images of H-MAA at pH = 6.5 at different times. Scale bar: 20 μm.

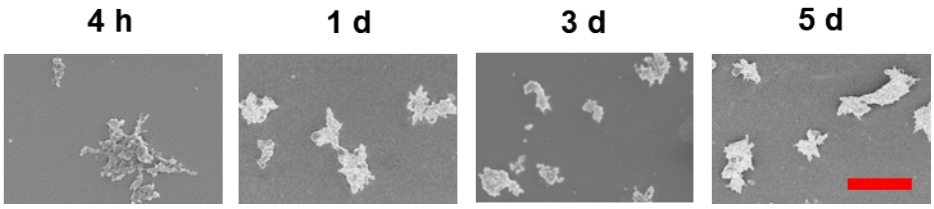

Fig. S23. The evaluation results on biodegradability of H-MAA. SEM images of H-MAA at pH = 7.4 at different times. Scale bar: 20 μm.

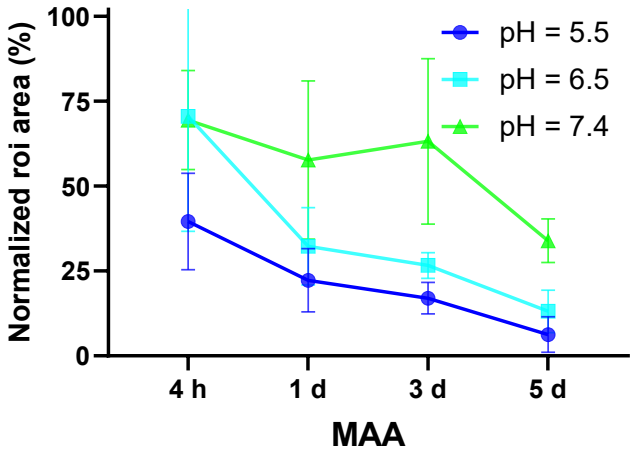

Fig. S24. A statistical analysis of ROI as observed through SEM by MAA.

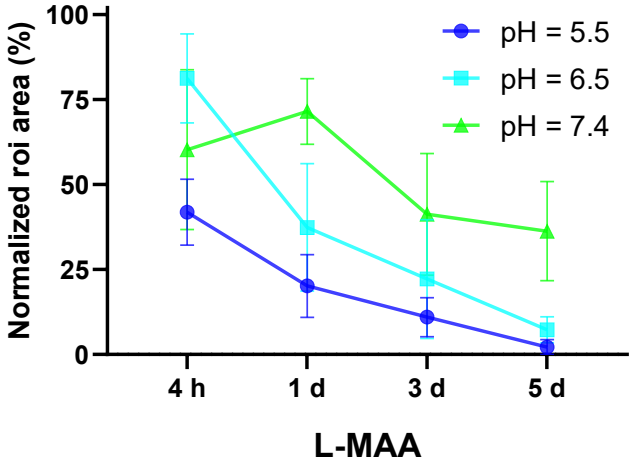

Fig. S25. A statistical analysis of ROI as observed by SEM of L-MAA.

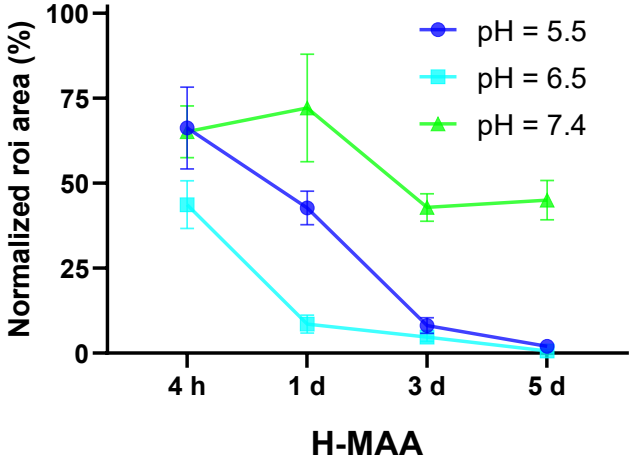

Fig. S26. A statistical analysis of ROI as observed by SEM of H-MAA.

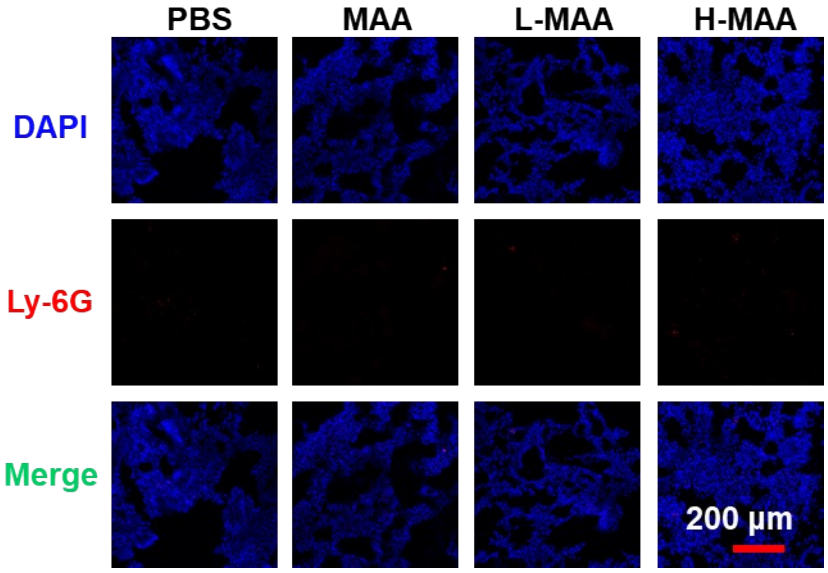

Fig. S27. Safety assessment of MAA and mineralized MAA (L-MAA and H-MAA). CLSM images of Ly-6G positive cells in lung from the mice after different treatments. Scale bar: 200 μm.

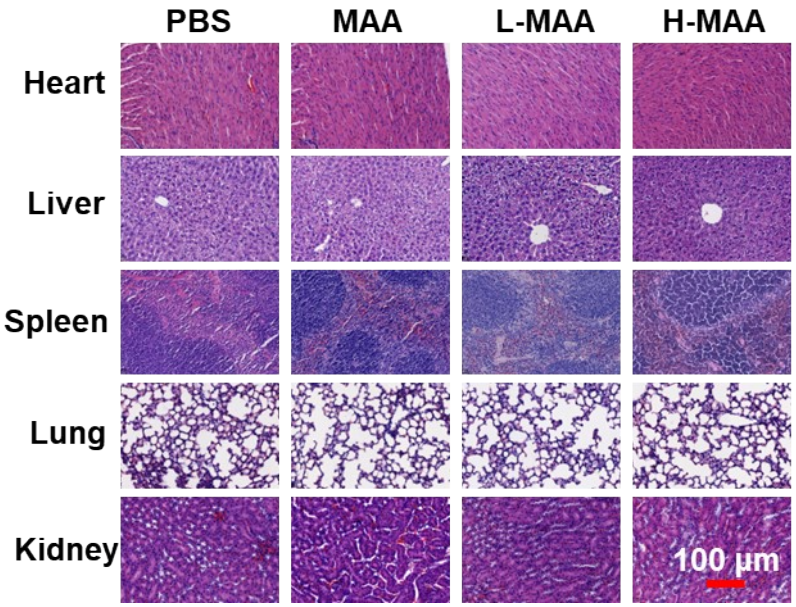

Fig. S28. H&E staining of main organs from the mice after different treatments.

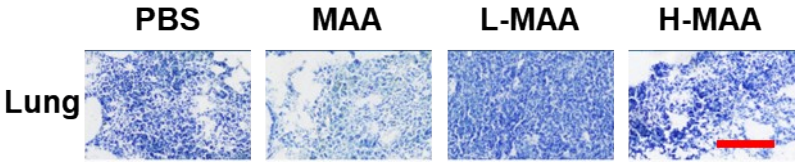

Fig. S29. Toluidine Blue O staining of lung tissues from the mice after different treatments. Scale bar: 100 μm.

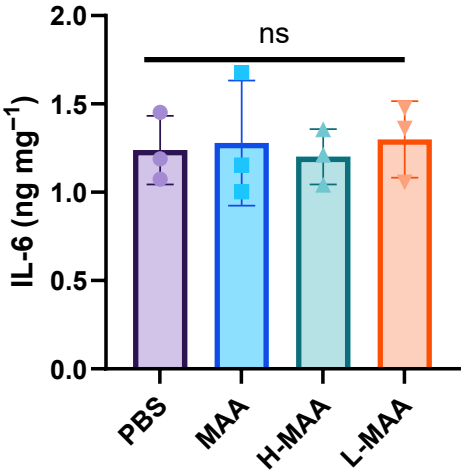

Fig. S30. Safety assessment of MAA and mineralized MAA (L-MAA and H-MAA). IL-6 in serum from the mice after different treatments.

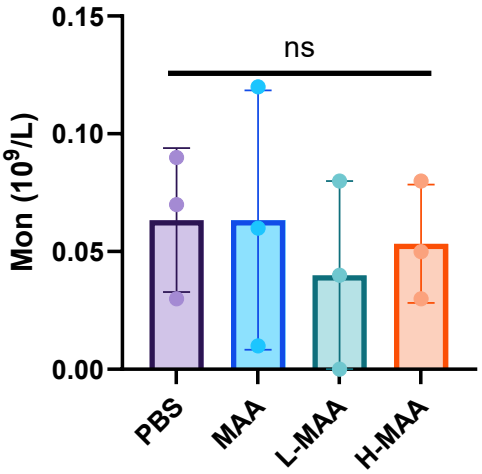

Fig. S31. Safety assessment of MAA and mineralized MAA (L-MAA and H-MAA). The levels of monocyte (Mon) in mice treated with PBS, MAA, L-MAA, and H-MAA, respectively.

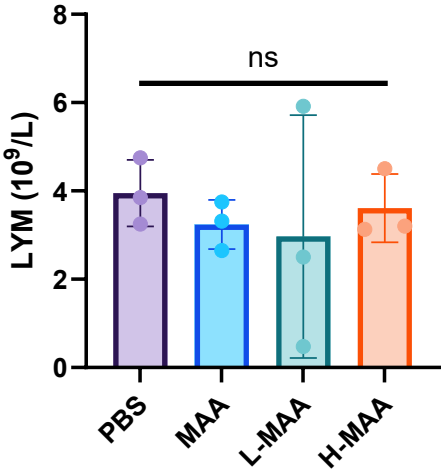

Fig. S32. Safety assessment of MAA and mineralized MAA (L-MAA and H-MAA). The levels of lymphocyte in mice treated with PBS, MAA, L-MAA, and H-MAA, respectively.

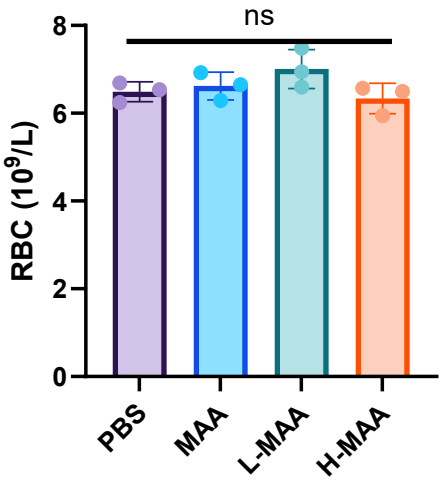

Fig. S33. Safety assessment of MAA and mineralized MAA (L-MAA and H-MAA). The levels of red blood cells (RBC) in mice treated with PBS, MAA, L-MAA, and H-MAA, respectively.

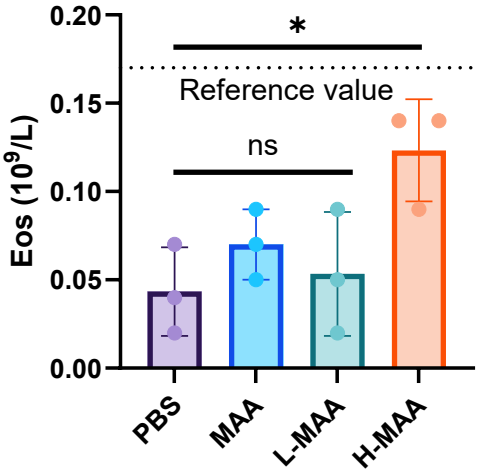

Fig. S34. Safety assessment of MAA and mineralized MAA (L-MAA and H-MAA). The levels of eosinophils (Eos) in mice treated with PBS, MAA, L-MAA, and H-MAA, respectively.

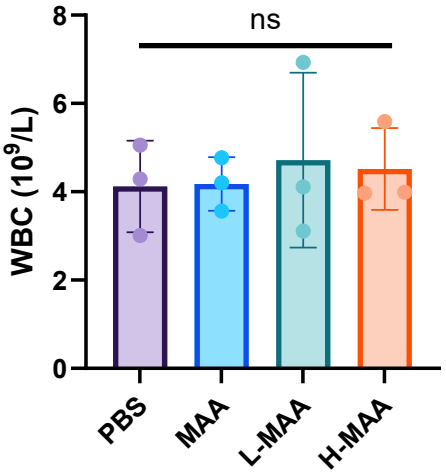

Fig. S35. Safety assessment of MAA and mineralized MAA (L-MAA and H-MAA). The levels of white blood cells (WBC) in mice treated with PBS, MAA, L-MAA, and H-MAA, respectively.

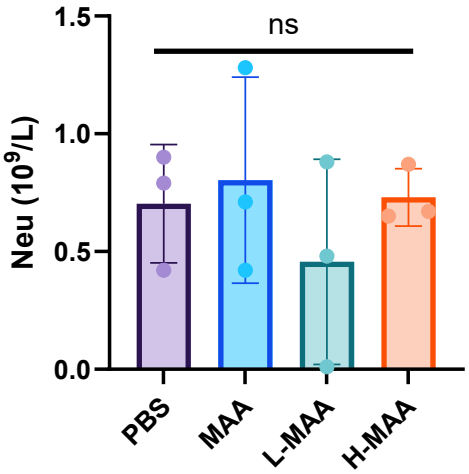

Fig. S36. Safety assessment of MAA and mineralized MAA (L-MAA and H-MAA). The levels of neutrophils (Neu) in mice treated with PBS, MAA, L-MAA, and H-MAA, respectively.

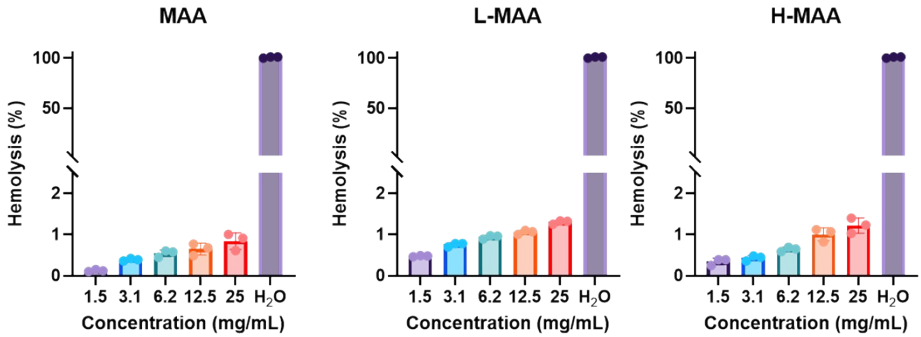

Fig. S37. The hemolysis results of MAA, L-MAA, and H-MAA.

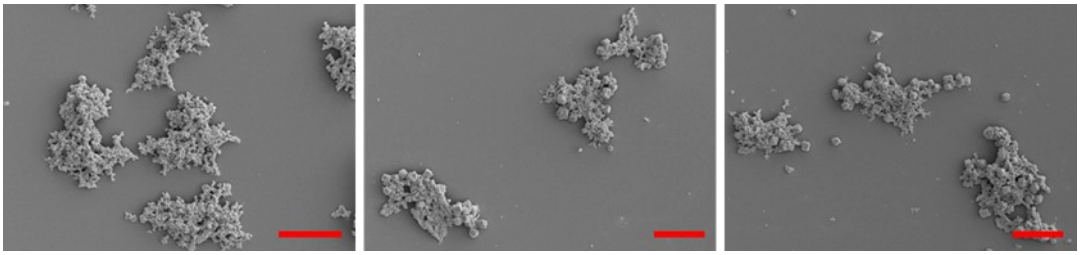

Fig. S38. The SEM images of MAA, L-MAA, and H-MAA in serum. Scale bar: 50 μm.

Reference

1. M. B. Giles, J. K. Y. Hong, Y. Liu, J. Tang, T. Li, A. Beig, A. Schwendeman and S. P. Schwendeman, *Nat. Commun.*, 2022, **13**, 3282.
2. J. Li, J. Xu, Y. Wang, Y. Chen, Y. Ding, W. Gao, Y. Tan, N. Ge, Y. Chen, S. Ge, Q. Yang, B. He and X. Ye, *Adv. Mater.*, 2024, **36**, e2405224.